Advancement in Medicinal Plant Research
Vol. 12(3), pp. 49-58, August 2024
DOI: 10.30918/AMPR.123.24.020
ISSN: 2354-2152
Full Length Research Paper

Andrographolide modulates *eNOS*-NO and Insulin-Glut4 signals of cultured lung epithelial and skeletal muscle cells

Jasadee Kaewsrichan[1*], Paweena Wongwitwichot[1] and Ashara Pengnoo[2]

[1]Department of Pharmaceutical Chemistry, Faculty of Pharmaceutical Sciences, Prince of Songkla University, Hat-Yai, Songkhla, 90112, Thailand.
[2]Division of Agricultural Innovation and Management, Faculty of Natural Resources, Prince of Songkla University, Hat-Yai, Songkhla, 90112, Thailand.

Accepted 13 August, 2024

ABSTRACT

Glucose metabolism and lung function have been affected by viral respiratory infections, leading to increased hospitalization and death of diabetic patients. In this study, cells from lung epithelium and skeletal muscle, A549 and C2C12 respectively, were cultured and treated with some used drugs (lopinavir, ritonavir, oseltamivir, and/or celecoxib) and andrographolide (ADP). The transcription of genes, including *il-6*, *tnf-α*, *inos*, *cox-2*, *enos*, *glut4*, and *irs-1*, was investigated using the Real-Time PCR method. Concerning gene translation levels, the activity of the phosphor-p65 transcription factor, the amount of GLUT4 protein expression, and the production of nitric oxide (NO) were quantified using a specific ELISA kit, western blotting method, and an enzymatic detection kit. *enos*-Transcription and NO-production were regulated in ADP-treated A549 cells. Modulations of *il-6*, *tnf-α*, and *inos* gene transcriptions, GLUT4 protein expression, and phosphor-p65 transcription factor activity were evident in C2C12 cells after ADP treatment. Using ADP as a drug adjuvant might be advantageous for diabetic patients infected with respiratory viruses due to its demonstration of anti-inflammatory and anti-hyperglycemic effects. These data might be applicable to formulating ADP tablets or nasal sprays for diabetes.

Keywords: Andrographolide, A549 cell line, C2C12 cell line, inflammatory genes, nitric oxide, NF-κB signaling pathway, GLUT4.

*Corresponding author. E-mail: jasadee.k@psu.ac.th. Tel: +66 89 7322235.

INTRODUCTION

Based on the clinical efficiency of using *Andrographis paniculata* and its major active, e.g., andrographolide (ADP), for curing respiratory tract infections caused by viruses for decades, there has been a recent interest of researchers to research more about molecular pharmacology and pharmacokinetics, as well as pharmaceutical stability of the active compound (Adiguna et al., 2021). It was noted that *A. paniculata* was dispensed as a component of the “Xiyanping” Chinese traditional recipe to most patients attacked by SARS-CoV-2 in China, to whom satisfactory treatments were acquired (Wang et al., 2021). In Vero cell culture, the killing of the infected SARS-CoV-2 by the herb’s extract was reported (Lim et al., 2021). By using computational approaches, several proteins of human infectious viruses were presumed as ADP-targets and commonly associated with attachment-, replication-, and spreading out-processes rendered by such pathogens (Kaewsrichan et al., 2024; Veerasamy and Karunakaran, 2022). An immune-modulating effect of ADP was additionally suggested by Rajanna et al. (2021). Therefore, using ADP to prevent influenza infection in healthy adults was evident (Rajanna et al., 2021).

In general, influenza infection causes mild symptoms of a disease called flu. However, people with comorbid conditions like obesity, chronic obstructive pulmonary

disease, vascular diseases, and diabetes may have higher risks of flu-related hospitalization and death (Costantini et al., 2021; Lina et al., 2020). Annual flu vaccination is thus recommended to vulnerable people by the World Health Organization to help them protect themselves from serious illnesses, while 100% protection cannot be expected. By the recent season (A.D.2024), the US-CDC have approved all nasal spray vaccines composed of quadrivalent influenza strains for flu vaccination of healthy, non-pregnant persons between 2 and 49 years of age. In regard to immune-compromised, older, or pregnant persons, another intramuscular or sub-cutaneous influenza vaccine can be applied instead. It is accepted that pains at injection sites and allergic reactions are major causes of repudiation to injecting vaccines. A decrease in mass compliance to such vaccination routes is a fair result (CDC, 2023).

Epithelial cells that line the respiratory tract may form an active barrier to sense any changes in the airway, and it is the first site to be assaulted by airborne pathogens and allergens. Once interactions between the barriers and uncommon matters are sensed, recruitment of cells of innate immunity is initiated, and the cells begin body protection (Kia'i and Bajaj, 2023). Adenosine triphosphate (ATP) is an important energy source for driving and supporting many cellular processes. Therefore, regular glucose metabolism of cells, especially of skeletal muscles, is essential for the acquisition of sufficient ATPs. In diabetes, complications like muscle fatigue and weakness are common, resulting from defective glucose uptake, glucose intolerance, and insulin insensitivity (Lien et al., 2018). These patients may have impaired immune responses and are susceptible to infections (Costantini et al., 2021). Accordingly, this work aimed to examine molecular targets of ADP in cells of lung epithelium and skeletal muscle, using A549 and C2C12 cells of ATCC cell lines, respectively. After incubated with a quadrivalent flu vaccine in high glucose (HG)-containing medium, data of cell treatments using ADP and other common drugs (e.g., lopinavir, ritonavir, oseltamivir and celecoxib) were compared. This would be helpful to develop pharmaceutical formulations containing ADP as an active for diabetes in the future.

MATERIALS AND METHODS

Drugs, reagents and antibodies

A pre-filled syringe influenza vaccine (Sanofi, UK) was obtained from the Pharmacy Department of PSU Hospital, Thailand. Other used items were ordered from distributors in the nation. Celecoxib (PHR1683), lopinavir (192725-17-0), ritonavir (155213-67-5), and oseltamivir phosphate (204255-11-8) were drugs used as positive controls and bought from Merck (Darmstadt, Germany). ADP was extracted from *Andrographis paniculata* grown under our previously established hydroponic system (Petty Patent No. 2303001648, Thailand) and standardized for the % authentic ADP according to the protocol of Thai Herbal Pharmacopoeia 2021 before use (Kaewsrichan et al., 2024). Recombinant human insulin (4 mg/ml) (2451703) was obtained from Gibco (NY, USA). BCA Protein Assay Kit, as well as chemicals and reagents for cell culture technique, such as fungizone, penicillin-streptomycin, trypsin, Trizol™ reagent, RIPA buffer, F-12K medium, Dulbecco's Modified Eagle's Medium (DMEM) (02854), DMEM high glucose (06492), and fetal bovine serum (FBS) were purchased from Thermo Fisher Scientific (MA, USA). A nitric oxide assay kit (MAK454) was bought from Sigma-Aldrich (Darmstadt, Germany). ELISA assay kits of COX-2 and NF-κB p65 transcription factor were acquired from RayBiotech Inc. (GA, USA). Primary antibodies against GLUT4 (ab33780) and β-actine (4970S) were obtained from Abcam (Singapore) and Cell Signaling Technology (MA, USA), respectively. HRP-linked secondary antibody (7074S) was bought from Cell Signaling Technology.

Test drug solutions

A stock solution of drugs, including lopinavir (10 mM in ethanol), ritonavir (6.6 mM in ethanol), oseltamivir (10 mM in water), celecoxib (2 mM in ethanol), and ADP (6.6 mM in methanol), was prepared and filtered through a 0.22-µm membrane filter before use. From tailored approaches, each solution was diluted to a final concentration by using a growth medium specific for a used cell line. These were 100 µM lopinavir and oseltamivir, 67 µM ritonavir, 67 and 80 µM ADP, 80 µM celecoxib, and 100 nM insulin.

Cell culture conditions

A549 is the human alveolar basal epithelial cell line of ATCC, which was normally maintained in 10% FBS containing F-12K medium. Also, C2C12 is a myoblast cell line from ATCC. The cells were commonly cultured in DMEM supplemented with 10% FBS. DMEM high glucose (HG-DMEM) was used to replace DMEM when specified. Routinely, these cells were grown in a CO_2 (5%) incubator, 95% relative humidity, 37^{O}C. After treatments, cells were either extracted for total RNA by using Trizol™ reagent or prepared as cell lysates by using RIPA buffer following the manufacturer's protocols.

The IC_{20} of a drug on A549 or C2C12 cells

The general MTT assay method was applied to determine

the IC_{20} of lopinavir, ritonavir, oseltamivir, celecoxib, and ADP on A549 and C2C12 cells. Cells of 95% confluency in a well of 96-well plates were separately incubated with a drug for 24 h using a concentration range between 0 and 300 µM. After the test solution was removed, MTT solution (5 mg/ml in PBS) of 100 µl was added and incubated in a CO_2 incubator for another 4 h and removed. Then, a 150-µl DMSO was added to dissolve the formazan product formed in live cells. OD_{570} data was collected by using a microplate reader. The percentage (%) of cell viability was calculated, while that of the untreated cells was considered as 100% viability.

Quantitative real-time PCR (qPCR)

cDNA-strands were synthesized in a 25-µl reaction mixture composed of SensiFAST™ cDNA Synthesis Kit reagent (Bioline, USA), oligo(dT)20 primer, and 500 ng RNA template for which thermal cycles of 25^{O}C, 10 min; 42^{O}C, 15 min, and 85^{O}C, 5 min were set-up. Of each sample, the qPCR experiment was done in triplicate on Magnetic Induction Cycler (Mic qPCR) (Bio Molecular Systems, Australia) using a temperature program of 95^{O}C, 5 min; 40 cycles of 95^{O}C, 30 sec and 60^{O}C, 1 min, and qRT-PCR Brilliant III SYBR Master Mix (Agilent, CA, USA). Genes to be investigated included *il-6*, *tnf-α*, *enos*, *inos*, *cox-2*, *glut4*, and *irs-1*. Oligonucleotide primers were obtained from Origene™ Technology, including MP206798 (*il-6*), MP217748 (*tnf-α*), NM_000603 (*enos*), NM_000625 (*inos*), NM_000963 (*cox-2*), MP215705 (*glut4*), MP206572 (*irs-1*), and MP200232 (*β-actin*). The primer specificity of a PCR product was confirmed by dissociation curve analysis. Data belonging to the *β-actin* gene were used for expression normalization. Expression of a tested gene was corresponded to the Ct value. After normalized with that of the *β-actin* gene and compared with that of the untreated control, relative gene expression in folds changed was reported.

Growing A549 cells in a conditioning medium

A549 cells of 80% confluency in T25 culture flasks were separately incubated with 0 µl, 75 µl, 150 µl and 250 µl of the flu vaccine (see Materials and Methods) for 24 h. The cultured supernatant (CS-0, CS-75, CS-150 and CS-250) was removed, filtered through a 0.22-µm membrane filter, and kept at -20^{O}C until use. One volume of a CS and 9 volumes of fresh growth medium were mixed to prepare a conditioning medium (CM) of CM-0, CM-75, CM-150 and CM-250. The effects of celecoxib and ADP towards *enos* and *cox-2* gene transcription and NO production after incubation of A549 cells with each of these CM were determined.

Western blot analysis

The protein concentration of cell lysate samples was determined by using the BCA Protein Assay Kit. A 100-µg protein per sample was separated on a 12.5% SDS-PAGE gel and electro-transferred to a PVDF membrane (Millipore, Germany). The membrane was blocked in TBS-tween for 4 h and incubated with 1^{O} antibodies (1:1000 dilution in TBS-tween) at 4^{O}C overnight. Excess 1^{O} antibodies were washed away by using TBS-tween. The membrane was next incubated with HRP-linked 2^{O} antibody (1:2000) for 1 h, followed by washing excess 2^{O} antibody away by using TBS-tween. An enhanced chemiluminescence kit (Millipore) was utilized for signal generation. Band visualization was done using Luminescent Image Analyzer (GE Healthcare, Sweden). Band density was computed by using ImageQuant™ TL 10.2 analysis software.

Nitric oxide (NO) assay

The assay of NO was based on the total amounts of NO_2^- and NO_3^- present in a sample, which were promptly obtained by the oxidation of NO. All existing NO_3^- species were reduced to NO_2^- by Griess reagent. The NO_2^- standard curve was constructed according to the kit's protocol and used to determine the NO concentration in a sample. This result was normalized with its corresponding protein concentration before reporting.

Determination of COX-2 enzyme synthesis

The enzyme COX-2 secreted by cells into cell supernatant was measured by using RayBio® COX-2 ELISA kit. A range of COX-2 standard solutions were prepared according to the kit's protocol. The standard and a test sample were separately added into wells of anti-COX-2 pre-coated plate, incubated for 2.5 h at room temperature, and removed. Then, biotin-linked anti-COX-2 antibody was added, followed by incubation for 1 h at room temperature with gentle shanking, and removed. Excess antibodies were washed away. HRP-conjugated streptavidin was added and incubated at room temperature for 45 min before removal. After complete washing, TMB solution was added for color development at room temperature for 30 min. The stop-solution was added, and the OD_{450} was measured immediately. The concentrations of COX-2 in samples were calculated by comparing with the standard curve.

Assay of NF-κB p65 transcription factor activity

The activity of the phosphor-p65 (p-p65) transcription

factor was monitored by using RayBio® NF-κB p65 Transcription Factor Activity Assay Kit. Samples of whole cell lysate were separately added into a well of NF-κB binding sequence (5′-GGGACTTTCC-3′) pre-coated plate, incubated at 4°C overnight, and removed. A specific p-p65 primary antibody was added and incubated for 2 h at room temperature. Unbound antibodies were washed away. Next, an HRP-conjugated secondary antibody was included, incubated for 1 h at room temperature, and removed. TMB Substrate Reagent was added for color development at room temperature for 1 h. The stop-solution was added, and the OD_{450} was immediately measured.

Statistical analysis

All data were reported as the mean ± S.D. Differences between groups were evaluated at $p = 0.05$ using the Student *t*-test or ANOVA with post hoc test Bonferroni of the IBM SPSS software for multiple comparisons.

RESULTS AND DISCUSSION

Cells treated with drugs at IC_{20}

Regarding the US-CDC guidelines, antiviral drugs such as lopinavir, ritonavir, and oseltamivir have been recommended for use in high-risk outpatients with suspected and confirmed influenza (CDC, 2023). To others who have had pulmonary inflammation, which resulted from robust immune responses to the infection, celecoxib has been dispensed (Villa-Hermosilla et al., 2022). There have been links between infectious influenza and inflammatory cytokines-mediated release (Kany et al., 2019). Therefore, the effects of ADP on transcriptions of *il-6*, *tnf-α*, *cox-2*, *inos*, and *enos* genes in A549 and C2C12 cells were prior investigated. Different drugs at concentrations inducing cell death by 20% (IC_{20}) were used for cell treatment. This was for obtaining maximum drug effect with minimum drug toxicity (Table 1). Skeletal muscle is comprehended as the major site of the body for glucose disposal, and deficiency of its role can be easily monitored according to insulin response and glucose tolerance of the tissue cells (Merz and Thurmond, 2020). To prove these, cells of C2C12 grown in a high glucose medium with a drug added were examined. In Figure 1, about 20% of the cells were destroyed using the IC_{20} of ADP, lopinavir or ritonavir. Then, growth disruption was not apparent for these three drugs. A slight growth promoting effect was suggested for oseltamivir, i.e., less than 20% of the cells were killed. It would be certain to consider the effects of drugs on gene transcription and protein expression together with glucose uptake ability and inflammation of C2C12 cells grown on high glucose medium.

Table 1. The IC_{20} (μM) of test drugs on A549 or C2C12 cells.

Test drug	IC_{20} (μM)	
	A549	C2C12
Lopinavir	ND	100
Ritonavir	ND	67
Oseltamivir	ND	100
Celecoxib	80	ND
Andrographolide	80	67

ND, not determined.

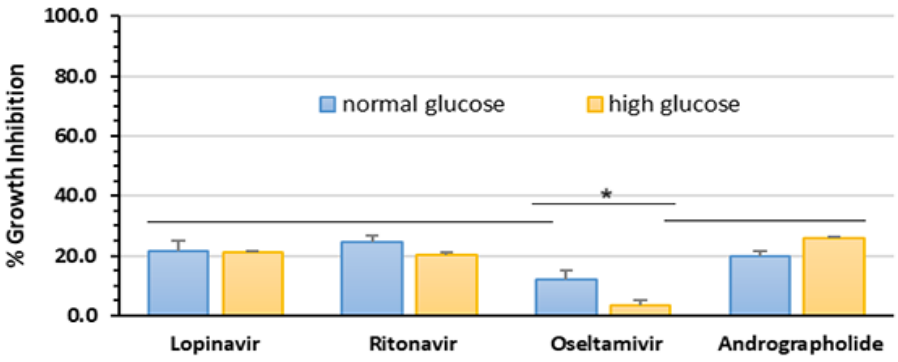

Figure 1. Effects of high glucose on the growth of C2C12 cells after treatments using lopinavir, ritonavir, oseltamivir and ADP at each corresponding IC_{20}, determined by MTT assay; *, $p < 0.05$.

Transcriptions of inflammatory genes in C2C12 treated cells

The transcriptions of genes including *il-6*, *tnf-α*, *cox-2*, *inos*, *enos*, *glut4*, and *irs-1* of C2C12 cells treated with lopinavir (100 µM), oseltamivir (100 µM), ADP (67 µM), or ritonavir (67 µM) for 24 h were investigated. In Figure 2, the levels of *il-6*, *tnf-α*, and *inos* transcripts in a normal glucose medium were found to increase with lopinavir, ritonavir, and ADP treatments. These were even increased for the cells grown in a high-glucose medium. On the contrary, *cox-2* transcription was decreased in both media by treatments using these three drugs. Significantly, transcriptions of *il-6*, *tnf-α*, *inos*, and *cox-2* genes in both media were not influenced by the oseltamivir challenge. In Figure 3, there were no changes of *irs-1* and *glut4* gene transcriptions after treatments using lopinavir, ritonavir, oseltamivir, and ADP in either normal- or high-glucose containing medium.

The activity of NF-κB p65 transcription factor of C2C12 treated cells

The NF-κB signaling is identified as a pivotal pathway in mediating inflammation through which immune cells are activated by infected pathogens, leading to the production and secretion of inflammatory cytokines such as IL-6 and TNF-α. Indeed, the pathway is driven by several transcription factors, but p65 is an important one (Guo et al., 2024). Under the non-activating stage, p65 bonds to IκB-protein, forming an inactive complex in cell cytoplasm. Upon activation, the secreted cytokines signal to degrade the bound IκB and release the p65. This p65 then forms a heterodimer with p50 and is translocated to the nucleus to bind to a specific response element of inflammatory genes downstream of the pathway. Aggressive production of inflammatory cytokines is the final result (Cesidio et al., 2018). The direct relationship between p65 transcription factor activity and inflammation has been established recently (Redd et al., 2015). Due to the increase of *il-6*, *tnf-α*, and *inos* transcripts of C2C12 cells treated with ADP in high glucose medium (Figure 2), it was rational to monitor the p65 transcription factor activity after drug challenges. In Figure 4a, inhibition of p65 transcription factor activity was higher for ADP-treated cells in a normal glucose medium compared to insulin treatment. The effect of insulin on inflammation inactivation has been consistently reported (Kaewsrichan et al., 2020). But, in a high glucose medium, the p65 activity was likely provoked by ADP and insulin challenges. Such activity induction was greater for insulin in comparison to ADP. Therefore, increased inflammation of C2C12 cells by insulin incubation in a high glucose medium was suggested. To know whether there was an impairment in the ability of glucose uptake of these inflamed cells, the expressed GLUT4 protein was measured by using the Western blotting technique. In Figure 4b, the protein was increasingly expressed by insulin-treated cells in a normal glucose medium, but this was decreased by ADP treatment. Notably, the effect of ADP and insulin on GLUT4 expression was reversed in high glucose medium, i.e., increased by ADP and decreased by insulin. In accordance, using ADP in diabetes might be suitable because of that glucose uptake could be facilitated due to the increased GLUT4 protein, resulting in improvement of insulin sensitivity and glucose tolerance of skeleton muscles (Wang et al., 2020).

Responses of A549 cells to the quadrivalent influenza vaccine and drugs

The structures and functions of epithelial cells that line the respiratory tract have been thoroughly characterized. This knowledge is applied to create different lung epithelial cell lines for screening and testing of matters passing through the airway to present effects (Miller and Spence, 2017). In consistence, the A549 lung epithelial cell line was recently used for the investigation of responses after incubated with a quadrivalent influenza vaccine and drugs (see Materials and Methods) (Salvemini et al., 2013; van der Vliet et al., 2000). COX-2 is a representative inflammatory marker of several lung diseases (Grace et al., 2021). However, measurements of *enos* and *cox-2* transcriptions, COX-2 enzyme activity, and NO production were currently performed. In Figure 5, NO of approximately 10.8, 10.6, 12.1, and 11.6 µM were determined for CS-0, CS-75, CS-150 and CS-250 supernatants to which a 24-h incubation using 0, 75, 150, and 250 µL vaccine was respectively conducted. The concentration produced by CS-0 cells was consistently considered as the baseline (Sharma et al., 2007). Accordingly, cell inflammation would be initiated by using the vaccine of 150 and 250 µL, and this was a dose-independent effect.

The impact of this existing NO on *cox-2* and *enos* gene transcriptions of fresh A549 cells were next investigated. A mixed medium containing one volume of each supernatant from CS-0, CS-75, CS-150, and CS-250 and nine volumes of fresh medium was prepared to result in a conditioning medium (CM) of CM-0, CM-75, CM-150, or CM-250, respectively.

With this 10-fold dilution, CM-0 and CM-75 were estimated to contain 1-1.1 µM NO and 1.1-1.2 µM for CM-150 and CM-250 (Figure 5). As such, there was a narrow range of NO concentrations therein. In using ADP or celecoxib at its corresponding IC_{20} to treat the cells grown in each CM for 24 h, it was found that folds changed of *cox-2* transcripts were ~1, disregarding whether the cells were treated or untreated (Figure 6a).

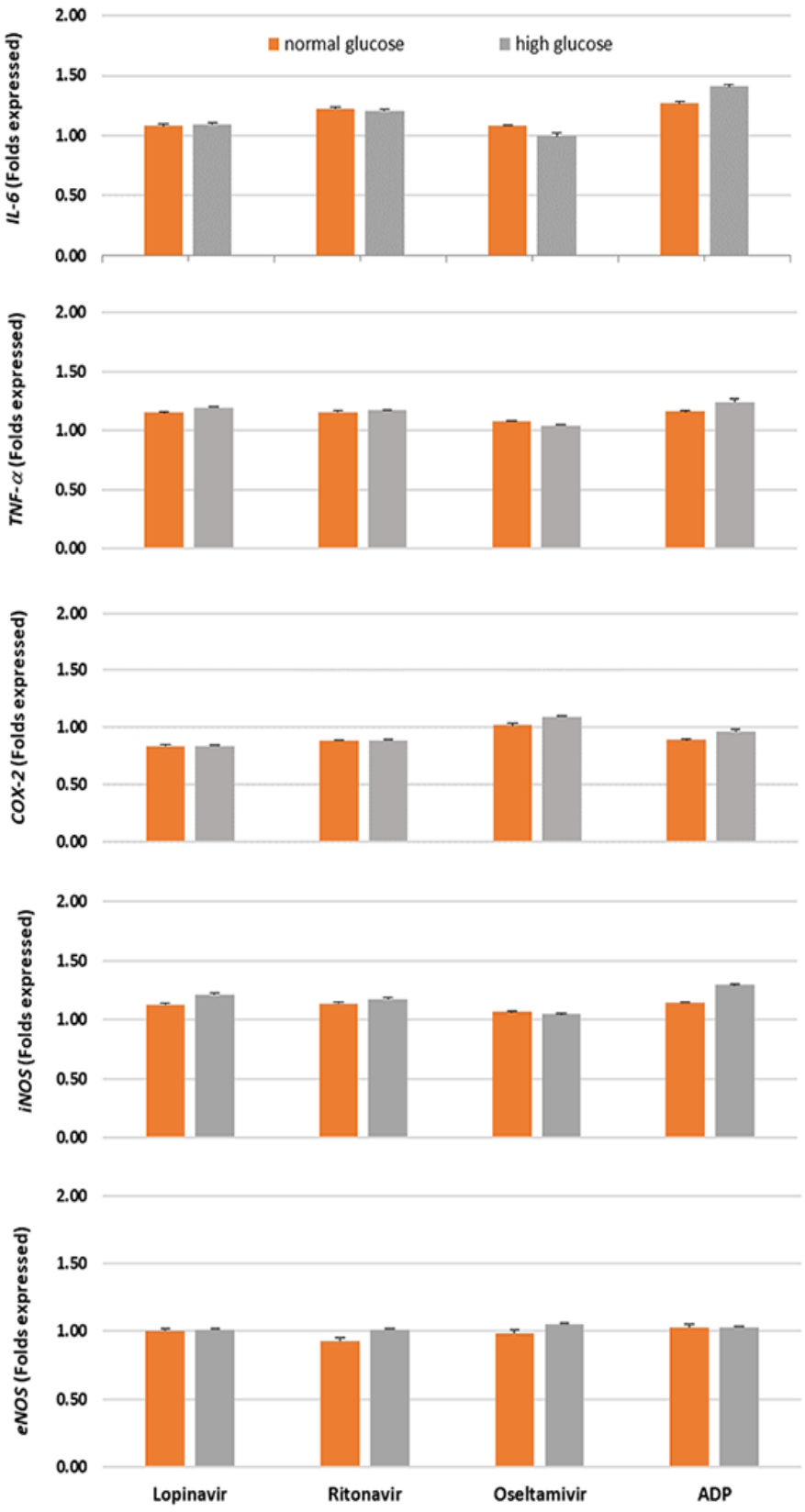

Figure 2. Transcriptions of *il-6*, *tnf-α*, *cox-2*, *inos* and *enos* genes of C2C12 cells grown in normal- or high glucose medium, determined by qPCR technique.

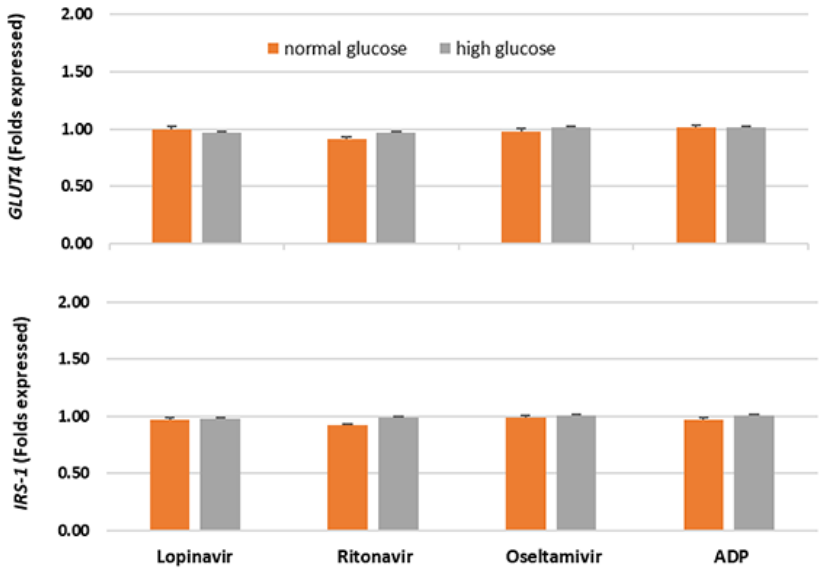

Figure 3. Transcriptions of *glut4* and *irs-1* genes of C2C12 cells grown in normal- or high- glucose medium, determined by qPCR method.

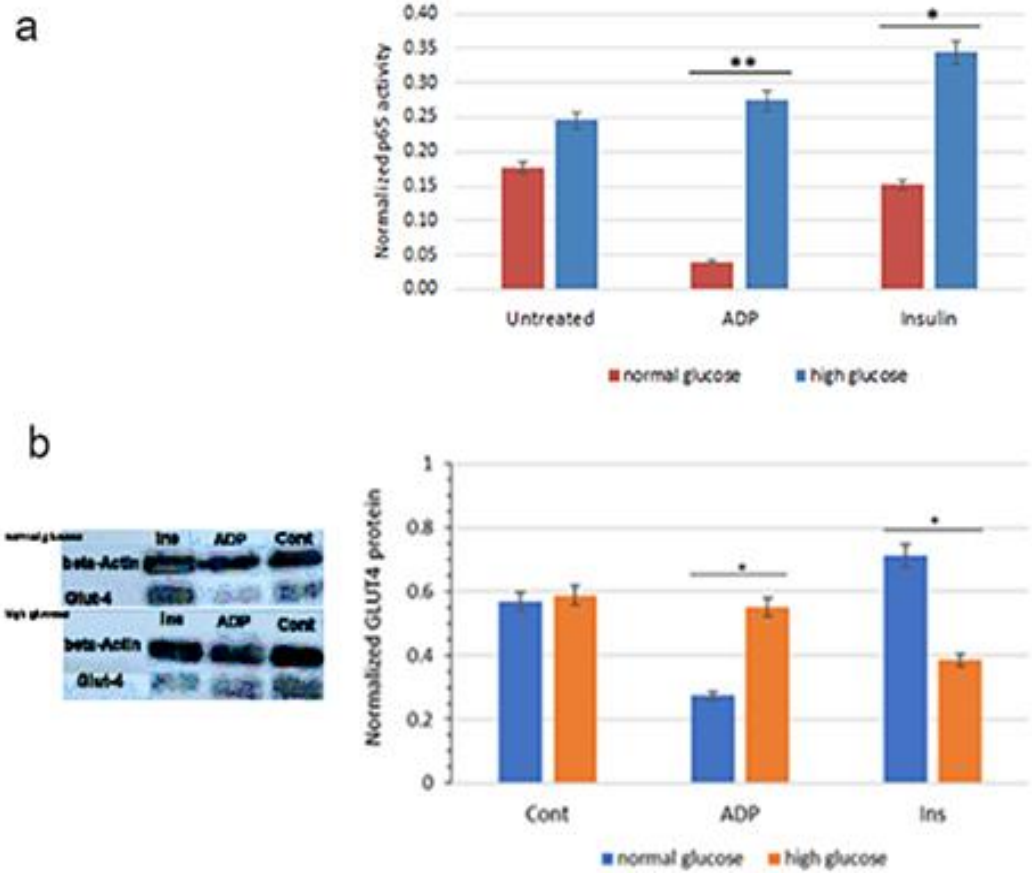

Figure 4. The p65 transcription factor activity (a) and the expressed GLUT4 protein (b) of C2C12 cells grown in normal- or high-glucose medium with ADP and insulin treatments for 24 h, determined by a specific assay kit (see Methods) and Western blotting technique, respectively; Ins, insulin; **, $p < 0.01$; *, $p < 0.05$.

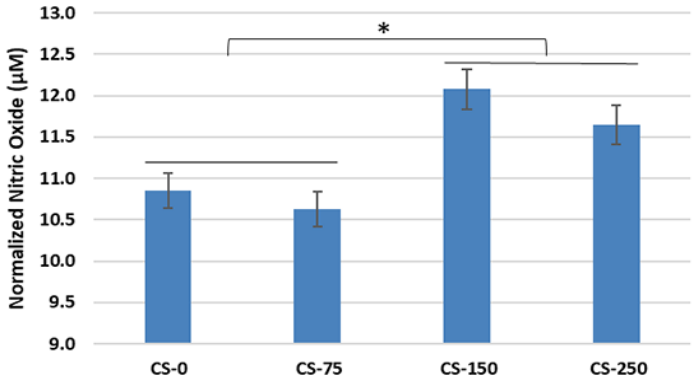

Figure 5. Production of NO by A549 cells after incubated with Sanofi ™ influenza vaccine of 0, 75, 150, or 250 μL for 24 h, determined in supernatant samples of CS-0, CS-75, CS-150 and CS-250, respectively; *, $p < 0.05$.

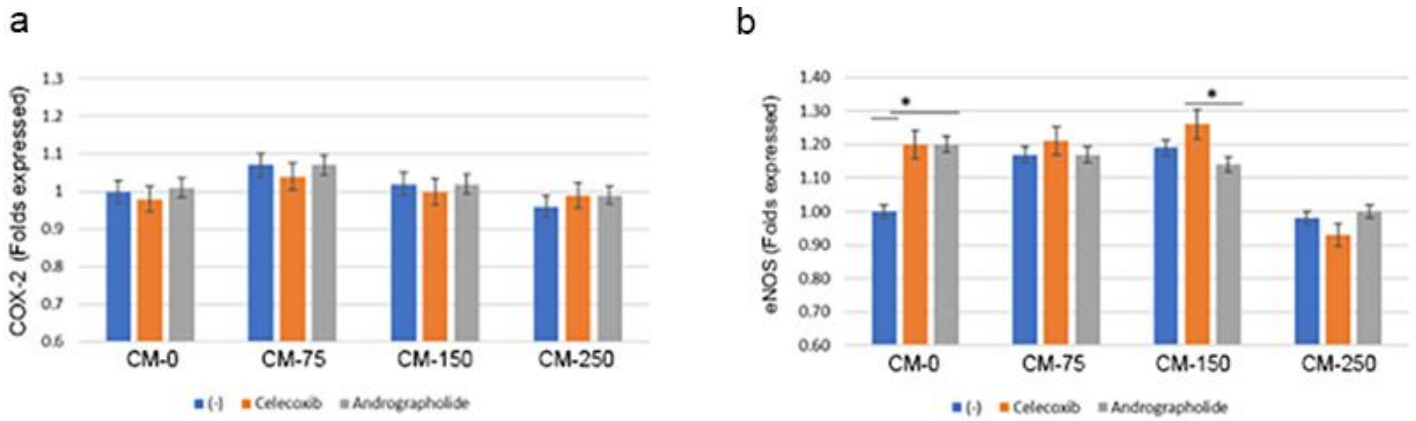

Figure 6. Transcriptions of *cox-2* (a) and *enos* (b) genes of A549 cells grown in CM-0, CM-75, CM-150 and CM-250 medium with or without drug treatment for 24 h, determined by qPCR method; *, $p < 0.05$.

That the drug treatment would solely affect protein expressions but not gene transcriptions was further clarified. Production of COX-2 protein in cell supernatants was then analyzed by using RayBio® COX-2 immunoassay kit. There were minor amounts of the enzyme found in CM-0, CM-75, CM-150 and CM-250 samples, which were lower than the LOQ of the kit (unpublished data). Consequently, it might not be suitable to predict the inflammation states of A549 cells by using COX-2 related signals, whether the gene transcription or the protein expression. Likewise, it would be doubtful for effective treatment of lung inflammation by using celecoxib. In Figure 6b, about 1.2 fold changes of *enos* transcription were calculated for CM-0, CM-75 and CM-250 samples after ADP and celecoxib treatments. For CM-75 and CM-150 cells, the gene transcripts were increased by about 1.2 folds even when treated. Notably, *enos* transcription was not altered for both treated and untreated CM-250 cells.

Regarding the difference in transcriptional activity of the *enos* gene of A549 cells, it was necessary to determine NO concentrations in culture supernatants again at the end of experiments. Respectively, about 13.1, 14.5, 13.9, and 13.5 μM NO were determined for CM-0, CM-75, CM-150, and CM-250 cells of non-drug treatment; 12.3, 11.6, 12.0, 12.3 μM NO of those challenged by celecoxib; and 13.1, 12.6, 12.4, 12.5 μM NO of those with ADP treatment (Figure 7). Therefore, NO of 10-12 μM would be the concentrations optimal for the growth and survival of A549 cells without inducing cellular oxidative stress and inflammation (Sharma et al., 2007). Using ADP and celecoxib might help balance NO production through transcriptional regulation of the *enos* gene of lung epithelial cells. Nevertheless, administrations of ADP and celecoxib would be useful for preventing inflammations of the airway in the future (Verheyen et al., 2022).

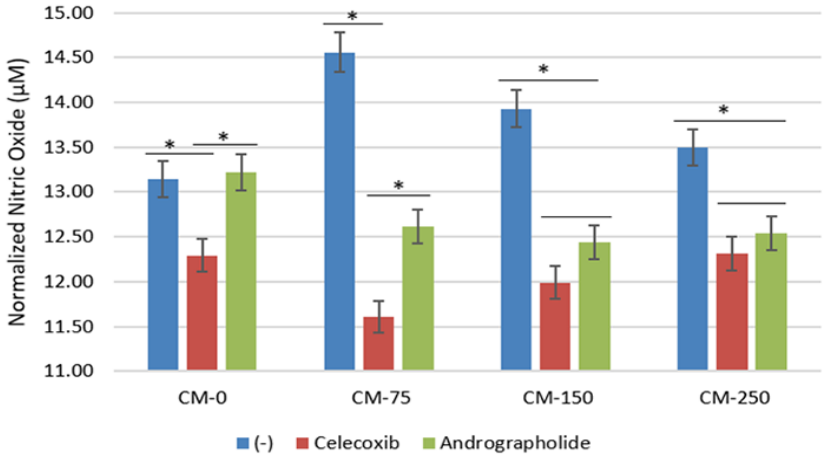

Figure 7. Production of NO by A549 cells grown in a conditioning medium of CM-0, CM-75, CM-150 and CM-250 with or without treatments using ADP or celecoxib for 24 h; *, $p < 0.05$.

In conclusion, ADP was shown to decrease *il-6*, *tnf-*α, and *inos* gene transcriptions and p65 transcription factor activity, as well as increase GLUT4 protein expression of skeletal muscle cells. Likewise, the effects of anti-inflammation and anti-diabetes were suggested. For diabetes, improvements in insulin sensitivity and glucose tolerance were implicated. Concerning its potential on epithelial cells of the respiratory tract, regulations of *enos* transcription and NO production were determined. The compound would be protective for airway injuries caused by excessive production of NO and inflammatory cytokines. It was interesting to develop pharmaceutical products containing ADP as an adjuvant or a drug substance for use in diabetes with influenza infection.

ACKNOWLEDGEMENT

The financial support was obtained from National Science, Research and Innovation Fund (NSRF) of PSU: FF2023-PHA6601118S.

REFERENCES

Adiguna SP, Panggabean JA, Atikana A, Untari F, Izzati F, Bayu A, Rosyidah AL, Rahmawati SI, Putra MY, **2021**. Antiviral activities of andrographolide and its derivatives: Mechanism of action and delivery system. Pharmaceuticals (Basel), 14(11): 1102. doi:10.3390/ph14111102.

Centers for Disease Control and Prevention; National Center for Immunization and Respiratory Diseases (NCIRD) (**CDC**), **2023**. Flu & Young Children. https://www.cdc.gov/flu/highrisk/children.html (Accessed on 10 January 2024)

Cesidio G, Ines B, Giorgio N, **2018**. The role of the transcription factor nuclear factor-kappa B in thyroid autoimmunity and cancer. Front Endocrinol, 9. https://www.frontiersin.org/articles/10.3389/fendo.2018.00471.

Costantini E, Carlin M, Porta M, Brizzi MF, **2021**. Type 2 diabetes mellitus and sepsis: state of the art, certainties and missing evidence. Acta Diabetologica, 58(9): 1139-1151. doi:10.1007/s00592-021-01728-4.

Grace VMB, Wilson DD, Siddikuzzaman RA, **2021**. Regulation of inflammation and COX-2 gene expression in benzo (a) pyrene induced lung carcinogenesis in mice by all trans retinoic acid (ATRA). Life Sci, 285: 119967. https://doi.org/10.1016/j.lfs.2021.119967.

Guo Q, Jin Y, Chen X, Ye X, Shen X, Lin M, Zeng C, Zhou T, Zhang J, **2024**. NF-κB in biology and targeted therapy: new insights and translational implications. Signal Transduct Target Ther, 9: 53. https://doi.org/10.1038/s41392-024-01757-9.

Kaewsrichan J, Wongwitwichot P, Manee S, **2020**. Health effects of ethanolic extract from seeds of lady finger. Food Health, 6(2): 90-97.

Kaewsrichan J, Wongwitwichot P, Tipmanee V, Pengnoo A, **2024**. Productive growing system of *Andrographis Paniculata* and inhibitions of reverse transcriptase and 3CLpro enzymes by the isolated andrographolide. Discov Agric Food Sci, 12(4): 21-34.

Kany S, Vollrath JT, Relja B, **2019**. Cytokines in inflammatory disease. Int J Mol Sci, 20(23): 6008. doi:10.3390/ijms20236008.

Kia'i N, **Bajaj** T, **2023**. Histology, Respiratory Epithelium. In: StatPearls [Internet]. Treasure Island (FL): StatPearls Publishing. https://www.ncbi.nlm.nih.gov/books/NBK541061/.

Lien AS, Hwang JS, Jiang YD, **2018**. Diabetes related fatigue sarcopenia, frailty. J Diabetes Investig, 9(1): 3-4. doi:10.1111/jdi.12752.

Lim XY, Chan JSW, Tan TYC, Teh BP, Mohd AR, Mohd R, Mohamad SSM, Ami F, **2021**. *Andrographis paniculata* (Burm. F.) Wall. Ex Nees, andrographolide, and andrographolide analogues as SARS-CoV-2 antivirals? A rapid review. Nat Prod Commun, 16(5). doi:10.1177/1934578X211016610.

Lina B, Georges A, Burtseva E, Nunes MC, Andrew MK, McNeil SA, Ruiz-Palacios GM, Feng L, Kyncl J, Vanhems P, Ortiz JR, Paget J, Reiner RC; GIHSN 2017–2018 study collaborators, **2020**. Complicated hospitalization due to influenza: results from the Global Hospital Influenza Network for the 2017-2018 season. BMC Infect Dis, 20(1): 465. doi: 10.1186/s12879-020-05167-4.

Merz KE, **Thurmond** DC, **2020**. Role of skeletal muscle in insulin resistance and glucose uptake. Compr Physiol, 10(3): 785-809. doi:10.1002/cphy.c190029.

Miller AJ, **Spence** JR, **2017**. *In vitro* models to study human lung development, disease and homeostasis. Physiology (Bethesda), 32(3): 246-260. doi:10.1152/physiol.00041.2016.

Rajanna M, Bharathi B, Shivakumar BR, Deepak M, Prashanth D, Prabakaran D, Vijayabhaskar T, Arun B, **2021**. Immunomodulatory effects of *Andrographis paniculata* extract in healthy adults - An open-label study. J Ayurveda and Integr Med, 12(3): 529-534. doi:10.1016/j.jaim.2021.06.004.

Redd P, Sharman S, Lu C, Yang D, Paschall A, Tulachan S, Liu K, **2015**. The NF-κB p65 and p50 homodimer cooperate with IRF8 to activate iNOS transcription. BMC Cancer, 15: 770. doi:10.1186/s12885-015-1808-6.

Salvemini D, Kim SF, Mollace V, **2013**. Reciprocal regulation of the nitric oxide and cyclooxygenase pathway in pathophysiology: relevance and clinical implications. Am J Physiol Regul Integr Comp Physiol, 304(7): R473-R487.

Sharma JN, Al-Omran A, Parvathy SS, **2007**. Role of nitric oxide in inflammatory diseases. Inflammopharmacology, 15(6): 252-259. doi:10.1007/s10787-007-0013-x.

van der Vliet A, Eiserich JP, Cross CE, **2000**. Nitric oxide: a pro-inflammatory mediator in lung disease? Respir Res, 1(2): 67-72. doi:10.1186/rr14.

Veerasamy R, **Karunakaran** R, **2022**. Molecular docking unveils the potential of andrographolide derivatives against COVID-19: an *in-silico* approach. J Genet Eng Biotechnol, 20: 58. https://doi.org/10.1186/s43141-022-00339-y.

Verheyen M, Puschkarow M, Gnipp S, Koesling D, Peters M, Mergia E, **2022**. The differential roles of the two NO-GC isoforms in adjusting airway reactivity. Am J Physiol Lung Cell Mol Physiol, 323(4): L450-L463.

Villa-Hermosilla MC, Negro S, Barcia E, Hurtado C, Montejo C, Alonso M, Fernandez-Carballido A, **2022**. Celecoxib Microparticles for Inhalation in COVID-19-Related Acute Respiratory Distress Syndrome. Pharmaceutics, 14(7):1392. doi: 10.3390/pharmaceutics14071392.

Wang C, Sun S, Ding X, **2021**. The therapeutic effects of traditional Chinese medicine on COVID-19: a narrative review. Int J Clin Pharm, 43: 35–45.

Wang T, Wang J, Hu X, Huang XJ, Chen GX, **2020**. Current understanding of glucose transporter 4 expression and functional mechanisms. World J Biol Chem, 11(3): 76-98. doi:10.4331/wjbc.v11.i3.76.

Citation: Kaewsrichan J, Paweena Wongwitwichot P, Pengnoo A, 2024. Andrographolide modulates *eNOS*-NO and Insulin-Glut4 signals of cultured lung epithelial and skeletal muscle cells. Adv Med Plant Res, 12(3): 49-58.